Kalman Filter for Noise Reduction and Dynamical Tracking for Levitation Control and for Plasma Mode Control

M. E. Mauel, D. Garnier, T. Pedersen, and A. Roach[†]

Dept. of Applied Physics

Columbia University

(† and MIT, Dept. Nuclear Engineering)

New York, NY 10027 USA

<mailto:mauel@columbia.edu>

November 10, 2004

Abstract. Feedback control is an important tool in fusion devices because it can lead to the control of instabilities and the optimization of plasma equilibria. For the Levitated Dipole Experiment (LDX), steady levitation of the floating superconducting coil requires an additional feedback control system. In this abstract, the active feedback control of the LDX floating coil is used to illustrate various digital algorithms for noise reduction and dynamical tracking. In particular, the recursive filter, now known as the "Kalman filter", is shown to be suitable for tracking the position, velocity, and acceleration of the floating coil. Using the measured power supply and known coil parameters, an adaptive Kalman filter is described that meets the requirements for levitation control. In addition, illustrations of the use of the Kalman filter for plasma instability control (like the resistive wall mode) are described.

- A real-time feedback control system (see Austin Roach, Tuesday afternoon's "Undergraduate Poster Session", `[FP1.039]`) will provide the safe and accurate positioning of the f-coil by controlling the currents in the superconducting I-coil and eight copper saddle coils.

- The I-coil acceptance tests were completed by Phil Michaels in the Summer of 2003. An analytical model was developed that includes inductive coupling to eddy currents flowing in the copper support plate. These eddy currents change the time-response of the levitation field to changing control voltages applied to the I-coil.

The question answered in this poster,"How should the LDX f-coil feedback control algorithm change as a result of the I-coil test data?"

Results and Summary

- Simple simulations of vertical feedback control that incorporate the new analytical model for the l-coil **only slightly modify** design requirements for the f-coil feedback controller.

- Because feedback control requires measurement of the f-coil's velocity and acceleration, **noise immunity requires careful filter design**.

- A Kalman filter is demonstrated, and **this filter meets LDX requirements**.

- Simulations of "loss-of-control" accidents also show that **previous designed protective measures will be adequate**.

Dynamical Equations for Inductive Feedback Control for the Vertical Motion of F-Coil

$$\frac{dz}{dt} = v_z \tag{1}$$

$$\frac{dv_z}{dt} \approx g(c-1) + \gamma^2 z \left(1 + \frac{z}{d_{z1}} + \left(\frac{z}{d_{z2}}\right)^2 + \left(\frac{z}{d_{z3}}\right)^3 + \ldots\right) \tag{2}$$

$$\frac{dc}{dt} = \frac{V}{L_l I_0} \tag{3}$$

$$V = G_p z^m + G_d \frac{dz^m}{dt} + G_{d2} \frac{d^2 z^m}{dt^2} \tag{4}$$

The three gain parameters are used to (i) define the equilibrium location, G_p, (ii) stabilize vertical displacements, G_d, and (iii) damping vertical oscillations, G_{d2}. They translate measurements of the f-coil position, $z^m \approx z$, into the control voltage, V, applied to the l-coil.

Definitions in Dynamical Equations for Inductive Feedback Control for the Vertical Motion of F-Coil

- $c \approx 1$ is the normalized levitation field

- $L_l I_0 \approx 680$ Volt·sec is the self-flux linked by the levitation coil at equilibrium.

- Eq. 3 represents an "ideal" l-coil magnet and power supply prior to Phil Michael's tests.

- Without feedback, the linear unstable growth rate for vertical displacements is γ, and the (weak) axial variation of the levitation force is expressed above as a Taylor series. For our base-case equilibrium (with the f-coil charged to 1.18 MA·turns, 103.7 A in the l-coil, and 16 A in the c-coil), $\gamma = 3.8$ s^{-1} when $c \approx 1$.

- For these calculations, we used 1500 lb, but now we've measured the final f-coil mass: 550 kg (1212 lb). Less levitation current is required.

- The weak axial variation is parameterized with $(d_{z1}, d_{z2}, d_{z3}) \approx (51, 82, 86)$ cm.

- The swing frequency for tilt motion is 0.9 Hz and for slide motion is 0.42 Hz. Tilt and slide swings are stable provided the f-coil is not less than 29 cm below nominal.

- These equations ignore f-coil flux conservation and dynamical coupling between f-coil degrees of freedom since these effects are not important for small displacements. Other equilibrium field configurations will have slightly different dynamical frequencies.

With $z_m = z$, the close-loop f-coil dynamics is described with a three-pole system

$$\frac{d^3z}{dt^3} = \frac{g}{L_l I_0}\left[G_p z + \left(G_d + \gamma^2\frac{L_l I_0}{g}\right)\frac{dz}{dt} + G_{d2}\frac{d^2z}{dt^2}\right] \tag{5}$$

When $G_p = 0$, the conditions for stability are easily solved. The derivative gains must satisfy

$$\eta_{fb} \equiv (-G_{d2})\frac{g}{2L_l I_0} \; > \; 0 \tag{6}$$

$$\omega_{fb}^2 \equiv (-G_d)\frac{g}{L_l I_0} - \gamma^2 - \eta_{fb}^2 \; > \; 0 \tag{7}$$

where η_{fb} is the closed-loop damping rate for f-coil displacements, ω_{fb} is the closed-loop vertical oscillation frequency. With $L_l I_0/g \approx 0.7$ Volt·s/(cm s^{-2}), the "acceleration gain" must be $(-G_{d2}) = 1.4$ to give $\eta_{fb} = 1$ s^{-1}. Stability requires the "velocity gain" (*i.e.* derivative gain) to be $(-G_d) \geq 10.8$ for this settling rate. When we add a small amount of proportional gain (in order to define the equilibrium f-coil position), an acceptable closed-loop response is $(G_p, G_d, G_{d2}) = (-1.0, -12.0, -1.7)$. This results in three damped modes with $\eta_{fb} > 0.65$ s^{-1} (and some residual oscillations with $\omega_{fb}/2\pi \approx 0.13$ Hz.)

The Need for Noise Reduction

- Derivative gain is highly susceptible to noise.

- The measured f-coil position must be filtered to keep the control voltage on the l-coil power supply to be be well within limits, ± 150 V.

- Voltage fluctuations cause small current oscillations that heat the l-coil.

These can minimized by filtering the output voltage of the feedback controller or by filtering the measurement data. The previous approach taken for an "ideal" L-coil was to apply the filter to the measurements.

Example Digitial Controller with Simple Averaging

For example, a digital controller with a sample period and latency both equal to $\delta t = 1$ ms. The measured positions of the f-coil (recorded at the *beginning* of each sample period) are z_n^m. Single pole filters are used to compute the position, $\bar{z}_n$, velocity $\bar{v}_n$, and acceleration, $\bar{a}_n$, used to output a voltage, $V_{n+1} = G_p \bar{z}_n + G_d \bar{v}_n + G_{d2} \bar{a}_n$, applied at the *end* of the sample period. Digital filters with unity DC gain are

$$\bar{z}_n = \bar{z}_{n-1} + \frac{\delta t}{\tau_z}(z_n^m - \bar{z}_{n-1}) \tag{8}$$

$$\bar{v}_n = \bar{v}_{n-1} + \frac{\delta t}{\tau_v}\left(\frac{(\bar{z}_n - \bar{z}_{n-1})}{\delta t} - \bar{v}_{n-1}\right) \tag{9}$$

$$\bar{a}_n = \bar{a}_{n-1} + \frac{\delta t}{\tau_a}\left(\frac{(\bar{v}_n - \bar{v}_{n-1})}{\delta t} - \bar{a}_{n-1}\right) \tag{10}$$

Integration times were equal to $\tau_z/\delta t = \tau_v/\delta t = 20$ and $\tau_a/\delta t = 50$. With z_n^m equal to the actual f-coil position plus "white noise" with a magnitude of ± 20 μm, the noise caused the output voltage to fluctuate about ± 3 V, and this drove fluctuations of the l-coil current at ± 10 mA. The power spectrum of the simulated l-coil current fluctuations are shown in Fig. 1. (If the filters shown in Eqs. 8-10 are removed, the voltage fluctuations are are approximately ± 5 kV!)
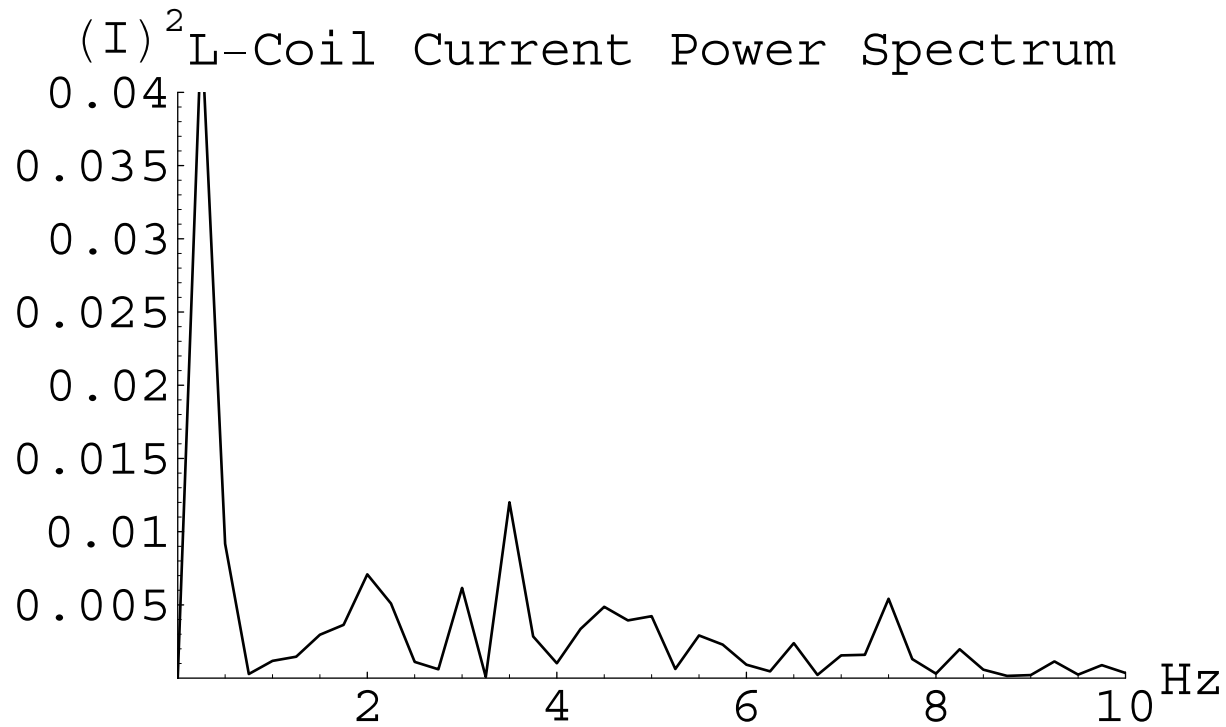
Figure 1

The DFT power spectrum from a simulation of the current fluctuations from an "**ideal**" I-coil due to ± 20 μm random measurement noise. The fluctuations of the I-coil current were acceptable: ± 10 mA.

The Empirical L-Coil Model

The measured response of the LDX l-coil to a voltage change couples the current through the superconductor to eddy currents in the support plate and currents passing through a short in the coil's insulation. The l-coil model is

$$
\begin{pmatrix} V \\ 0 \\ 0 \end{pmatrix} = \begin{pmatrix} L_l & M_{ls} & M_{lp} \\ M_{ls} & L_s & M_{sp} \\ M_{lp} & M_{sp} & L_p \end{pmatrix} \cdot \begin{pmatrix} \dot{I}_l \\ \dot{I}_l + \dot{I}_s \\ \dot{I}_p \end{pmatrix} + \begin{pmatrix} Q_l - R_s & R_s & 0 \\ 0 & Q_s + R_s & 0 \\ 0 & 0 & R_p \end{pmatrix} \cdot \begin{pmatrix} I_l \\ I_l + I_s \\ I_p \end{pmatrix}
$$

where Q_l and Q_s represent frequency dependent loss factors empirically determined from the AC l-coil test.

The levitation field results from the l-coil current, I_l, shielded by eddy currents in the support plate, I_p, and by eddy currents in the LDX vacuum chamber. Eq. 3 must be modified to incorporate these effects. Defining c_{vac} to be the control field at the f-coil *in the absence* of the LDX vacuum vessel, and setting $\tau_{vac} \sim 15$ ms (*e.g.* the value from the SPARK code), the new dynamical control equation is

$$
c = c_{vac} - \tau_{vac} \frac{dc}{dt} = \frac{I_l}{I_0} + \frac{2 I_p}{2796 I_0} - \tau_{vac} \frac{dc}{dt} \tag{11}
$$

where we used the number of turns in the l-coil (2796) and the effective "turns" in the support plate (2, for both sides) is used to compute C_{vac}.

Since $L_p/R_p \approx 0.3$ s is comparable to time-scales of interest, analysis of l-coil response is best done numerically. Nevertheless, it is useful to note the inductive limit of Eq. 11 when $I_p \approx -I_l M_{lp}/L_p = -1016 I_l$. In this case, an "equivalent" to Eq. 3 can be written as

$$\frac{dc}{dt} \approx \frac{V}{L_l I_0} \frac{1 - 2M_{lp}/2796 L_p}{1 - M_{lp}^2/L_l L_p} - \tau_{vac} \frac{d^2 c}{dt^2} \tag{12}$$

On the ~ 0.1 s time-scale, the voltage required to change the control flux changes only slightly: from ~ 680 Volt·sec for a "bare" l-coil to $\sim I_0 L_l \left(1 - M_{lp}^2/L_l L_p\right)/(1 - 2M_{lp}/2796 L_p) \approx 335$ Volt·sec for a "real" coil.

On slightly longer time scales, $\sim L_p/R_p$, the l-coil control flux, c_{vac}, is partially proportional to the l-coil voltage. The plate eddy currents act to "integrate" the l-coil current. The fact that $V \propto c_{vac}$ (instead of dc_{vac}/dt) over some time-scales necessitates additional proportional gain, G_p, for closed-loop stability.

Simple Digitial Controller with Time-Averaging Fails

The Laplace transform of Eqs. 1, 2, 4, 11, and 12 gives six poles (and one unstable mode, $\exp(\gamma t)$, when $G_p = G_d = G_{d2} = 0$.) The same gain vector discussed previously, $(G_p, G_d, G_{d2}) = (-1.0, -12, -1.7)$, stabilizes the f-coil using a "real" l-coil, but damps vertical displacements about 5 times more slowly, $\eta_{fb} > 0.11$ s^{-1}. Adjusting the gain vector with additional proportional gain, decreases the the settling time. When $(G_p, G_d, G_{d2}) = (-10, -17, -3.0)$, then $\eta_{fb} > 0.5$ s^{-1}. The primary consequence of the support plate eddy currents is to require an increase in the gain vector.

If the digital controller discussed in the previous section is employed with the new gain vector and "real" l-coil model, the performance deteriorates. With $\delta t = 1$ ms and a f-coil position noise of ± 20 μm, the fluctuation in the l-coil current increases nearly 10-fold to ± 91 mA. The fluctuating l-coil current power spectrum is shown in Fig. 2, illustrating both the increased noise amplitude and bandwidth. Additionally, the higher gain vector and larger number of (stable) poles makes the translation from the Laplace transform (analog) response to the digital (Z transform) response more problematic. For this example controller, the vertical displacements were underdamped–even though the analog response was nearly critical.
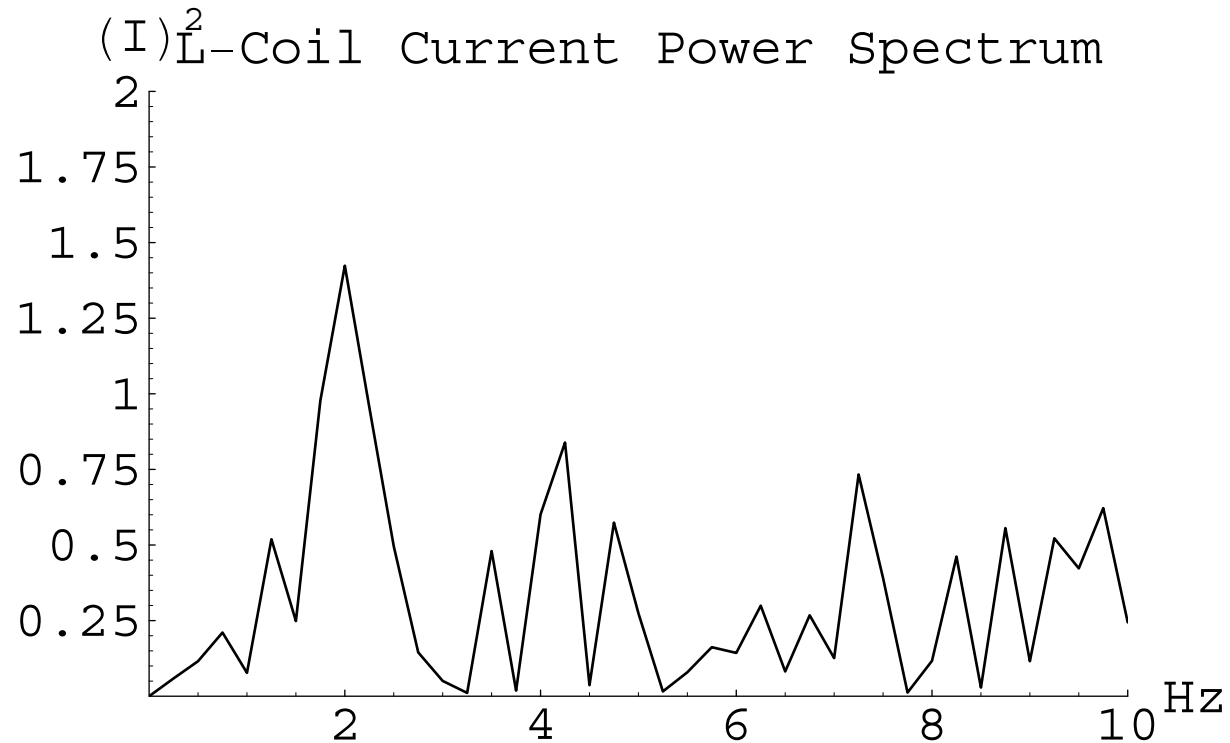
Figure 2.

The DFT power spectrum from a simulation of the I-coil current fluctuations including the effects from plate eddy currents, the I-coil short, and vacuum vessel eddy currents. **The current fluctuations increased significantly (from Fig. 1) to ± 91 mA.**

Rudolf Emil Kalman (May 19, 1930 -) is most famous for his invention of the Kalman filter, a mathematical digital signal processing technique widely used in control systems and avionics to extract meaning (a signal) from chaos (noise).

Kalman's ideas on filtering were initially met with scepticism. He had more success in presenting his ideas, however, while visiting Stanley Schmidt at the NASA Ames Research Center in 1967. This led to the use of Kalman filters during the Apollo program.

He was born in Budapest, Hungary. He obtained his bachelor's (1953) and master's (1954) degrees from MIT in electrical engineering. His doctorate (1957) was from Columbia University. His worked as Research Mathematician at the Research Institute for Advanced Study, in Baltimore, from 1958-1964, Professor at Stanford University from 1964-1971, and Graduate Research Professor, and Director, at the Center for Mathematical System Theory, University of Florida, Gainesville from 1971 to 1992. Starting in 1973, he simultaneously filled the chair for Mathematical System Theory at the Swiss Federal Institute of Technology, (ETH) Zurich.

He received the IEEE Medal of Honor (1974), the IEEE Centennial Medal (1984), the Inamori foundation's Kyoto Prize in High Technology (1985), the Steele Prize of the American Mathematical Society (1987), and the Bellman Prize (1997).

He is a member of the National Academy of Sciences (USA), the National Academy of Engineering (USA), and the American Academy of Arts and Sciences (USA). He is a foreign member of the Hungarian, French, and Russian Academies of Science. He has many honorary doctorates.

The Kalman Filter

A simple Kalman filter can remove most of the measurement noise of the f-coil position and allow straight-forward application of the gain vector during position feedback control. The Kalman filter is applied in two steps: the "prediction" or time update step and the "correction" or measurement update step.

For the f-coil control problem, I choose to model the "state" of the f-coil's position with a vector $\mathbf{x}_n \equiv \{z_n, z_{n-1}, z_{n-2}\}$, where z_n is the vertical position during the nth time-sample of the digital controller. The "prediction" step is an internal model describing how the f-coil advances one time-step from $\mathbf{x}_n$ to $\mathbf{x}_{n+1}$. A second-order accurate state map is

$$
\begin{aligned}
\mathbf{x}_{n+1} &= \begin{pmatrix} z_{n+1} \\ z_n \\ z_{n-1} \end{pmatrix} = \begin{pmatrix} \gamma^2 \delta t^2 + 2 & -1 & 0 \\ 1 & 0 & 0 \\ 0 & 1 & 0 \end{pmatrix} \cdot \begin{pmatrix} z_n \\ z_{n-1} \\ z_{n-2} \end{pmatrix} + \begin{pmatrix} g\delta t^2(I_l(n)/I_0 - 1) \\ 0 \\ 0 \end{pmatrix} \\
&\equiv \mathbf{A} \cdot \mathbf{x}_n + \mathbf{u}_n
\end{aligned}
$$

where $I_l(n)/I_0$ is the measured normalized current in the l-coil, and $\mathbf{A}$ is called the "process matrix".

The "correction" step involves computation of the "Kalman gain", $\mathbf{K}_n$ and using this matrix to weight the *residual* between the prediction and the measurement, z_n^m, of the f-coil. The Kalman gain is computed recursively along with the "estimate error covariance", $\mathbf{P}_n$. The estimate error covariance is related to the degree that measurement fluctuations differ

from the internal state vector. The Kalman gain is the matrix that minimizes *on average* the corrected error covariance.

In order to compute the Kalman gain, the relationship between the state vector, $\mathbf{x}_n$, and measurement needs to be defined. In this example, the relationship is trivial. If $\mathbf{z}_n^m \equiv \{z_n^m, z_{n-1}^m, z_{n-2}^m\}$, then $\mathbf{x}_n = \mathbf{H} \cdot \mathbf{z}_n^m$, with $\mathbf{H}$ equal to the identity matrix.

The two-step Kalman filter can now be defined. The "prediction" step is

$$
\begin{align}
\mathbf{x}_n^* &= \mathbf{A} \cdot \mathbf{x}_{n-1} + \mathbf{u}_n \tag{13} \\
\mathbf{P}_n^* &= \mathbf{A} \cdot \mathbf{P}_{n-1} \cdot \mathbf{A}^T + \mathbf{Q} \tag{14}
\end{align}
$$

where $\mathbf{x}_n^*$ and $\mathbf{P}_n^*$ are predictions of the next step state vector and error covariance. (The matrix $\mathbf{Q}$ is user-defined parameter for the intrinsic noise in the f-coil dynamics (for example, due to fluctuating stray fields in the cell or to vibrations of the f-coil vessel with respect to its conductor). For the simulations described here, I took $\mathbf{Q}$ to be small: the identity matrix $\times 10^{-5}$.) The "correction" step is

$$
\begin{align}
\mathbf{K}_n &= \mathbf{P}_n^* \cdot \mathbf{H}^T \cdot (\mathbf{H} \cdot \mathbf{P}_n^* \cdot \mathbf{H}^T + \mathbf{R})^{-1} \tag{15} \\
\mathbf{x}_n &= \mathbf{x}_n^* + \mathbf{K}_n \cdot (\mathbf{z}_n^m - \mathbf{H} \cdot \mathbf{x}_n^*) \tag{16} \\
\mathbf{P}_n &= (\mathbf{I} - \mathbf{K}_n \cdot \mathbf{H}) \cdot \mathbf{P}_n^* \tag{17}
\end{align}
$$

With $\mathbf{H} = \mathbf{H}^T = \mathbf{I}$ Eqs. 18-20 are especially simple. Even with a more complicated measurement matrix (*e.g.* when we use multiple laser detectors to simultaneously measure tilt, slide, and vertical position), these equations are less complicated than the sequential application of single-pole digital filters used in the example of the previous section.

The "Correction" Step and Control Computation

The "correction" step contains the important matrix, $\mathbf{R}$, called the "**measurement noise covariance**" matrix. This matrix is used by the filter designer to control the evolution of the state vector. When $\mathbf{R}$ is large, the process state is less sensitive to noise fluctuations. When $\mathbf{R}$ is small, the state vector's response is more sensitive to measurement noise. For the simulations I performed, I took $\mathbf{R}$ to be the identity matrix times a single parameter. This is appropriate if the noise for each measurement is independent or each other.

The final step in the digital controller is to compute the control voltage to be applied to the I-coil power supply. A second order formula is

$$V_n = \left(\begin{array}{ccc} G_p & G_d & G_{d2} \end{array} \right) \cdot \left(\begin{array}{ccc} 1 & 0 & 0 \\ 1/\delta t & -1/\delta t & 0 \\ 1/\delta t^2 & -2/\delta t^2 & 1/\delta t^2 \end{array} \right) \cdot \mathbf{x}_n \qquad (18)$$
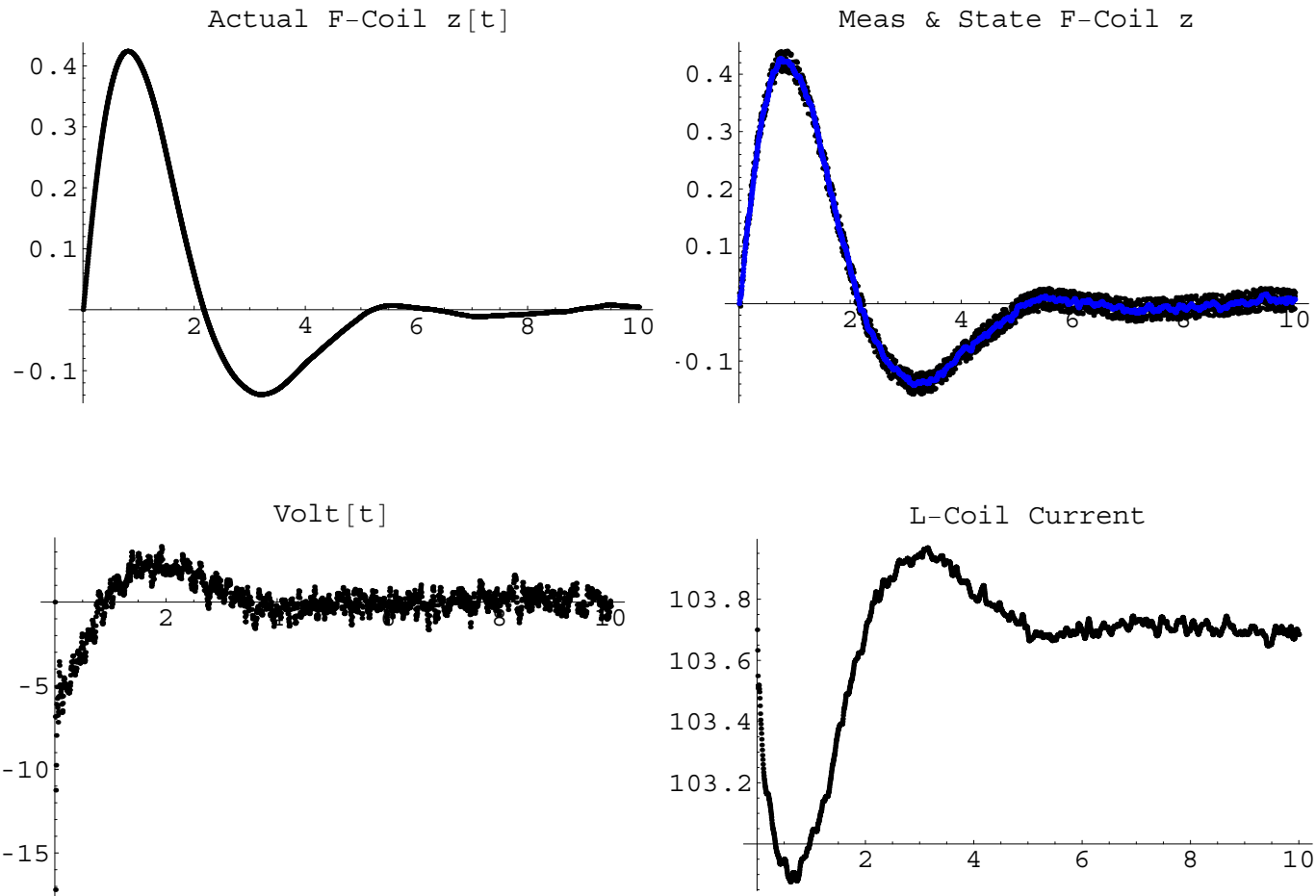
Figure 3. Simulation of F-coil position control using a digital controller and a Kalman filter. ("**Wow!**")
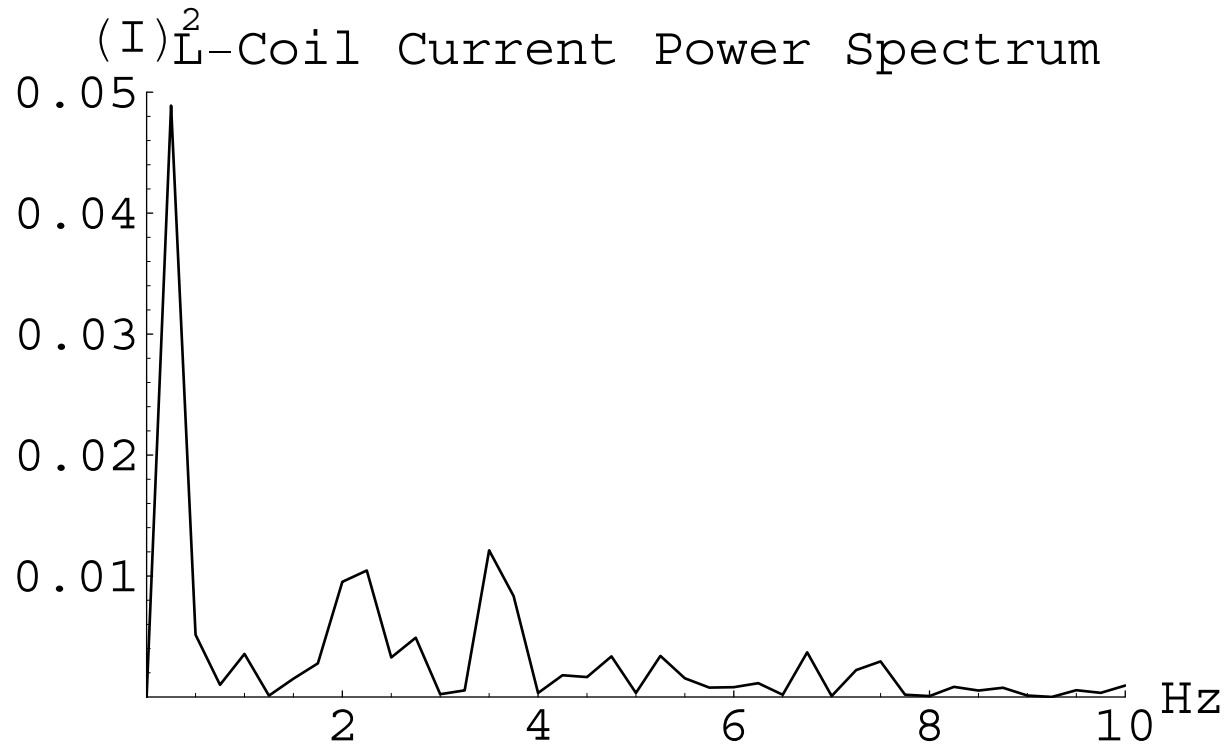
Figure 4.

The DFT of the I-coil current fluctuations from a simulation of the digital control of f-coil using a Kalman filter with $\mathbf{R} = \mathbf{I} \times 1$.
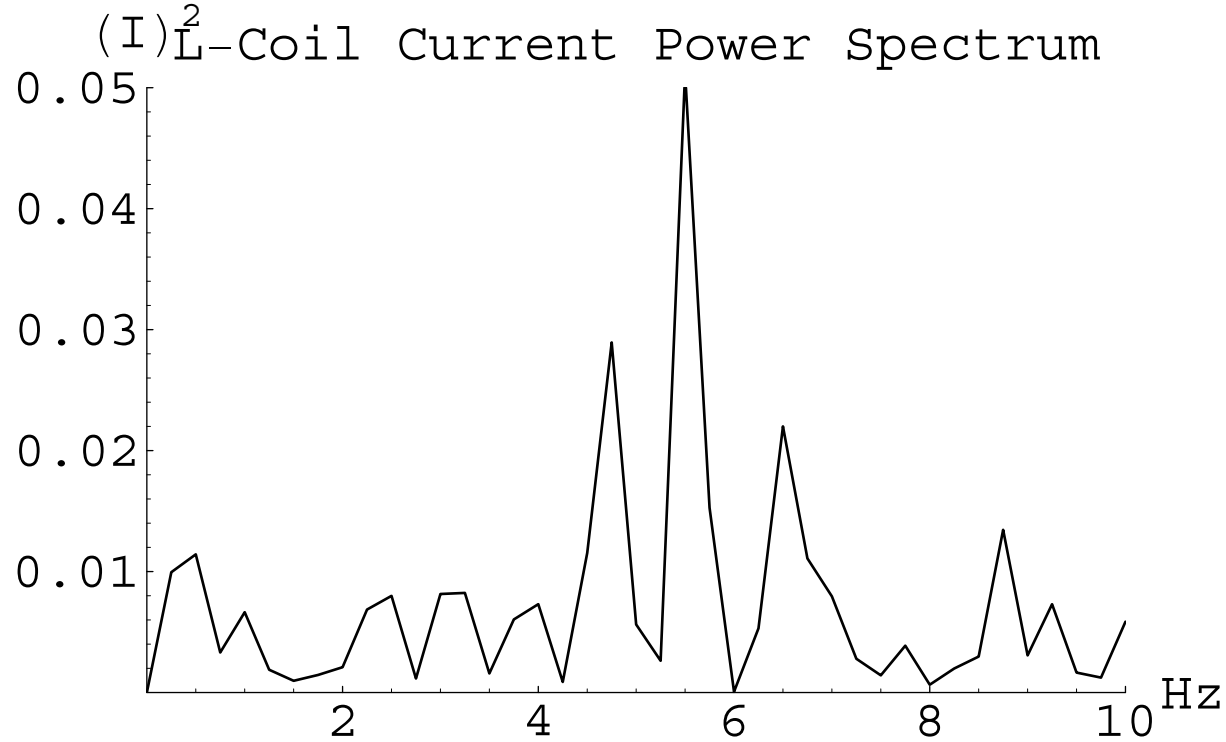
Figure 5.

The DFT of the I-coil current fluctuations from a simulation of the digital control of f-coil using a Kalman filter with $\mathbf{R} = \mathbf{I} \times 0.1$. The I-coil current fluctuations have increased to ± 29 mA.

Simulations show Kalman filter meets our requirements

Fig. 3 shows the response of the f-coil and the feedback system following an "instantaneous" step in the f-coil velocity. At $t = 0$, the f-coil's upward velocity is set to be 1 cm/s. The controller operated with a sample period of $\delta t = 5$ ms, and the tuning parameter was set to unity: $\mathbf{R} = \mathbf{I} \times 1$. The f-coil returned to equilibrium in about 5 s, comparable to the response obtained with an ideal analog controller. The steady fluctuations of the I-coil current had a standard deviation of ± 19 mA, but with a power spectrum dominated by low-frequencies, < 1 Hz, as shown in Fig. 4. With these filter/controller settings, the I-coil current fluctuations are nearly the same as obtained with a "bare" I-coil (shown in Fig. 1.) If the tuning parameter is made smaller, $\mathbf{R} = \mathbf{I} \times 0.1$, then the I-coil current fluctuations increase to ± 29 mA, and the power-spectrum has higher-frequency components, as shown in Fig. 5.

Loss of Control Accidents

- Another important requirement for the I-coil levitation system is rapid dump of the I-coil current in the event of a loss-of-control accident. The I-coil current must decrease sufficiently fast to prevent the upward acceleration of the f-coil to the I-coil.

- Simulations of loss-of-control accidents when a 2.5 Ω dump resistor is connected with the I-coil power supply. The f-coil response is essentially unchanged between a "bare" ($L_l = 6.6$ H) and "real" I-coil. The bottom two figures show the I-coil voltage and currents.
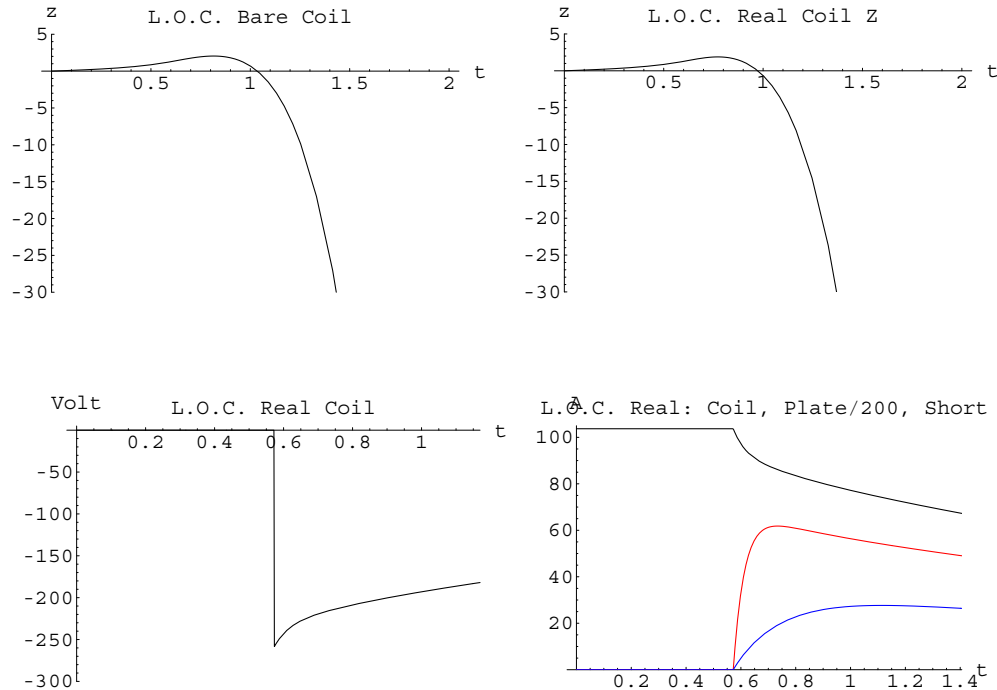
Figure 6. Comparison of the response of the f-coil during an example "loss-of-control" accident for a "bare" l-coil and a "real" l-coil. The f-coil is set to have an upward velocity of 1 cm/s, and the feedback controller is assumed to have failed. The "bare" coil has an inductance of 6.6 H; whereas, the effective inductance of the "real" coil is lower. The voltage on the l-coil power supply is initially zero. When the f-coil has moved upward by 1 cm, the l-coil is dumped through a 2.5 Ω resistor after a trigger delay of 35 ms. In Phil Michael's model, the resistance of the short, R_s, increases from 0.15 Ω to 1.5 Ω. Fig. 6 shows that the f-coil response remains essentially unchanged with the new l-coil model. If the f-coil is caught after falling to -30 cm, a constant 5-g catching force stops the f-coil in 2.4 cm after 31 ms.

Summary

- Vertical dynamics of the f-coil was re-examined using the empirical model of the actual I-coil.

- Using computer simulations, an active feedback controller using an adaptive Kalman filter was described that meets our requirements.

- Simulations of possible "loss-of-control" accidents shows that plans to dump the current in a "real" I-coil with 2.5 Ω resistor will prevent excessive upward motion of the f-coil.

References

- B. Y. Youngblood and D. Garnier, "A Model for Vertical Motion of LDX Floating Coil after Loss of Feedback Control," LDX-MIT-BY-070600-01, (2000).

- T. S. Pedersen, *et al.*, "Computer simulations and design of levitation feedback control system for the LDX," APS-DPP Meeting, (October, 2000).

- T. S. Pedersen, "LDX Feedback Control Simulations with Noise," LDX-CU-TSP-120800-01, (2000).

- D. Garnier, *et al.*, "Levitation Control System for the Levitated Dipole Experiment," APS-DPP Meeting, (October, 2001).

- A. L. Radovinsky, "F-Coil Vertical Position Control using a Field Sensor," LDX-MIT-ALRadovinsky-110102-02, (2002).

- T. S. Pedersen, "Specifications for TSP Power Supplies," LDX-CU-TSP-010402-01, (2002).

- P. Michael, "AC Test Results for the LDX L-Coil at 17 K," LDX-MIT-PMichael-062403-01, (2003).

- P. Michael, "Initial DC Operation of the LDX L-Coil," LDX-MIT-PMichael-062703-01, (2003).

- P. Michael, "L-Coil Emergency Discharge Experiment," LDX-MIT-PMichael-070803-01, (2003).

- P. Michael, "Analytical Model for L-Coil Behavior," LDX-MIT-PMichael-082503-01, (2003).

- P. Michael, "Implications from the L-Coil Analytical Model," LDX-MIT-PMichael-082503-01, (2003).

- P. Michael, *et al.*, "Performance of the Cryocooler-Cooled LDX Levitation Coil," CEC-ICMC Meeting, (2003), to appear in *Advances in Cyrogenic Engineering*.

- See extensive documentation and tutorials at
  `http://www.cs.unc.edu/~welch/kalman/`.